



OPEN ACCESS

EDITED BY

Ajaya Bhattarai,
Tribhuvan University, Nepal

REVIEWED BY

Bidyut Saha,
University of Burdwan, India
Mihalj Posa,
University of Novi Sad, Serbia

*CORRESPONDENCE

Yibo Zhou,
✉ zhoub@iim.ac.cn

RECEIVED 14 August 2024

ACCEPTED 16 September 2024

PUBLISHED 30 September 2024

CITATION

Shen Z and Zhou Y (2024) Effect of sodium dodecyl sulphate on the rheological and carbon sequestration properties of cemented paste backfill with CO₂ injection. *Front. Earth Sci.* 12:1480706. doi: 10.3389/feart.2024.1480706

COPYRIGHT

© 2024 Shen and Zhou. This is an open-access article distributed under the terms of the [Creative Commons Attribution License \(CC BY\)](https://creativecommons.org/licenses/by/4.0/). The use, distribution or reproduction in other forums is permitted, provided the original author(s) and the copyright owner(s) are credited and that the original publication in this journal is cited, in accordance with accepted academic practice. No use, distribution or reproduction is permitted which does not comply with these terms.

Effect of sodium dodecyl sulphate on the rheological and carbon sequestration properties of cemented paste backfill with CO₂ injection

Zhuo Shen and Yibo Zhou *

Information Institute of the Ministry of Emergency Management of the People's Republic of China, Beijing, China

Cemented paste backfill (CPB) is a technology that has a positive impact on both the environment and mining safety. In recent years, it has been widely applied and developed. To improve the carbon sequestration efficiency of CPB, air-entraining agent addition to CO₂-injected CPB (CO₂-CPB) has been proposed. However, the influence of air-entraining agents on the rheological and carbon sequestration properties of CO₂-CPB has not been investigated to date. Therefore, sodium dodecyl sulphate (SDS), an air-entraining agent, was selected in this study, and the rheological and carbon sequestration properties of CO₂-CPB added with SDS were comprehensively investigated. CO₂-CPB samples with 0.0%, 0.5%, 1.0%, and 1.5% SDS were prepared, and the rheological parameters (yield stress and viscosity) were tested after curing for 0, 0.25, 1, and 2 h. Gas content testing, microscopic analysis, and zeta potential measurements were performed. The results show that SDS addition decreased the yield stress and viscosity of CO₂-CPB at 0–1 h; however, the yield stress and viscosity increased at 2 h. SDS addition significantly improved the carbon sequestration performance of CO₂-CPB. The findings of this study have important implications for carbon sequestration development in CPB and solid waste utilisation.

KEYWORDS

tailings, carbon sequestration, sodium dodecyl sulphate, cemented paste backfill, rheology, mining

1 Introduction

The mining industry provides the raw materials needed for industrial development, in turn providing important support for global economic growth (Carvalho, 2017; Farjana et al., 2019; Qi, 2020). Currently, the manufacturing industry still has a high demand for ores, and the mining industry has vast potential for future development (Hu et al., 2016; Sánchez and Hartlieb, 2020; Yilmaz, 2023). Mineral resource mining can lead to several environmental protection problems, such as land subsidence and tailing accumulation (Marimuthu et al., 2021; Mohsin et al., 2021; Song et al., 2023; Tuokuu et al., 2019).

With the gradual depletion of shallow, easy-to-mineralise ores, the environmental protection problems faced by deep mining are becoming increasingly significant. Cemented paste backfill (CPB) is gradually becoming the mainstream green mining method because

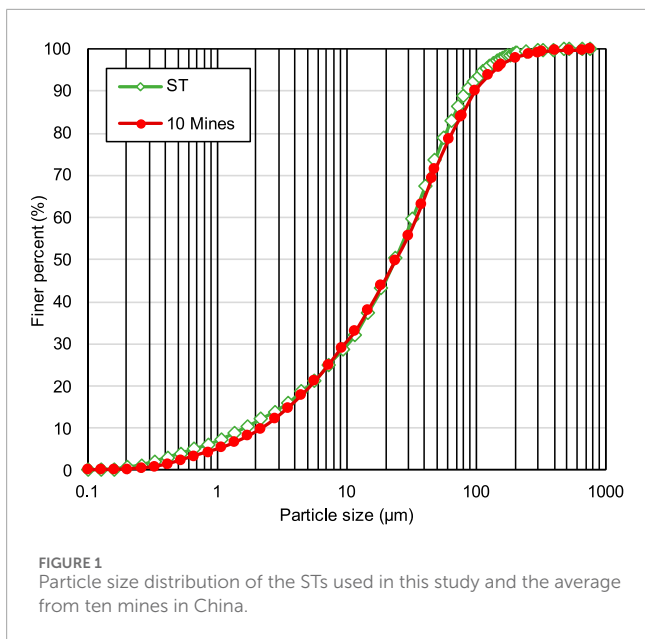


TABLE 1 Physical properties of the tailings.

Element /Unit	Gs/-	D ₁₀ /µm	D ₃₀ /µm	D ₅₀ /µm	D ₆₀ /µm
Silica tailings	2.7	1.7	9.8	23.9	32.1
Ten-mine average tailings	—	2.2	9.7	23.7	34.5

of its positive effects on roadway control, solid waste treatment, and ore recovery rate (Khandani et al., 2023; Sari et al., 2023; Sun et al., 2018). CPB, a backfill slurry composed of tailings, binders, water, and admixtures, has become the main management method for mine waste (Lu et al., 2024; Sheshpari, 2015; Wilson et al., 2018). CPB is filled into the underground mining area along with the pipeline to deal with solid waste and ensure roof plate stability. With the support of environmental awareness and national policies, backfill mining has gradually become safe, environmentally friendly, and efficient (Eker and Bascetin, 2022; Solismaa et al., 2021; Thompson et al., 2012; Yin et al., 2023).

With the development of global industry, a large amount of CO₂ has been emitted into the atmosphere, resulting in climate change and even extreme natural disasters (Adedoyin et al., 2020; Cassia et al., 2018). Therefore, the rational storage of CO₂ is an urgent research topic (Farajzadeh et al., 2020; Yamada, 2021). To reduce atmospheric CO₂ concentrations, CO₂ carbonation has been widely used to prepare new cement-based materials in recent years (Lippiatt et al., 2020; Ma et al., 2022; Olajire, 2013; Winnefeld et al., 2022). There is a large amount of waste space in mining goafs; therefore, carbon sequestration via mining backfill has become a popular research field (Ji and Yu, 2018; Uliasz-Bocheńczyk and

Mokrzycki, 2020). In the mining backfill process, CO₂ is filled into the CPB materials to undergo mineralisation reactions and achieve CO₂ sequestration in the CPB (Unluer, 2018; Wang et al., 2019; Xu and Ma, 2024).

Currently, there are two main backfill carbon sequestration process types. One is to conduct CO₂ to the mining goaf after the initial CPB solidification. Chen et al. (2022) simulated the engineering environment on backfill specimens using carbonation maintenance, compared and analysed the peak strength and hydration product differences between normal and carbonation maintenance specimens, and investigated the PH value of the carbonation degree of specimens of the two types of maintenance methods, which illustrates the effect of CPB carbon sequestration. The reaction rate can be increased by increasing the temperature and pressure. (Ćwik et al., 2018; Mo et al., 2016). found that a high temperature and pressure environment accelerated the CPB carbonation process; however, the increase of this type of method leads to construction management complexities and increased backfill costs, and the difference between the carbonation degree of specimens after carbonation conditioning and that of the natural conditioning may not be obvious. Another carbon sequestration method involves CO₂ injected into the CPB slurry. Ngo et al. (2023) used the bubbling method to prepare backfill specimens; that is, CO₂ was pumped into the slurry for 20 min and then placed into a mould for maintenance, along with the rheological properties of the slurry and the peak strength at different curing ages. They found that the viscosity of the slurry increased after CO₂ incorporation, which reinforced its early strength. However, for CO₂ carbonation, the abovementioned methods are limited in terms of time and efficiency. In other words, the carbon sequestration efficiency of CPB has not been fully utilised.

To improve the carbon sequestration efficiency and CPB time, we propose the addition of an air-entraining agent to a CO₂-injected CPB slurry (CO₂-CPB). Owing to the effect of the air-entraining agent, a large amount of CO₂ exists in the form of small bubbles in the CO₂-CPB, which can not only effectively increase the contact area between CO₂ and the CPB slurry, making carbon sequestration more efficient, but these small bubbles can also exist in the entire CPB transportation and curing processes, greatly extending the CO₂ mineralisation time. Furthermore, the presence of small bubbles in the CPB slurry can play a role in ball lubrication, which significantly improves the slurry's flow performance (Hefni and Hassani, 2021; Ouyang et al., 2008; Yang et al., 2022). However, to date, there are no reported studies on the influence of air-entraining agents on the rheological and carbon-sequestration properties of CO₂-CPB.

There are many types of air-entraining agents for cement-based materials, such as rosin resin, alkyl aromatic sulfonate, and soap (Gagné, 2016; Markiv, 2022; Mendes et al., 2017; Zhou et al., 2024). According to the previous research literature (Kundu et al., 2023; Kundu et al., 2024; Yang et al., 2022), sodium dodecyl sulphate (SDS) is a kind of air entraining agent that is easy to obtain and has excellent gas entraining effect. Therefore, to address the aforementioned technical gaps, the yield stress and viscosity of CO₂-CPB with SDS were experimentally investigated in this study. Additionally, the influence of the SDS on the carbon-sequestration efficiency of CO₂-CPB was investigated.

TABLE 2 Specific mineral composition and properties of Type I silicate cement.

Element	CaO	Al ₂ O ₃	SiO ₂	MgO	Fe ₂ O ₃	Others	Relative density/kg·m ⁻³	Specific surface area/m ² ·kg ⁻¹
Type I silicate cement (%)	65.08	5.53	22.36	1.27	3.46	2.30	3,115	350

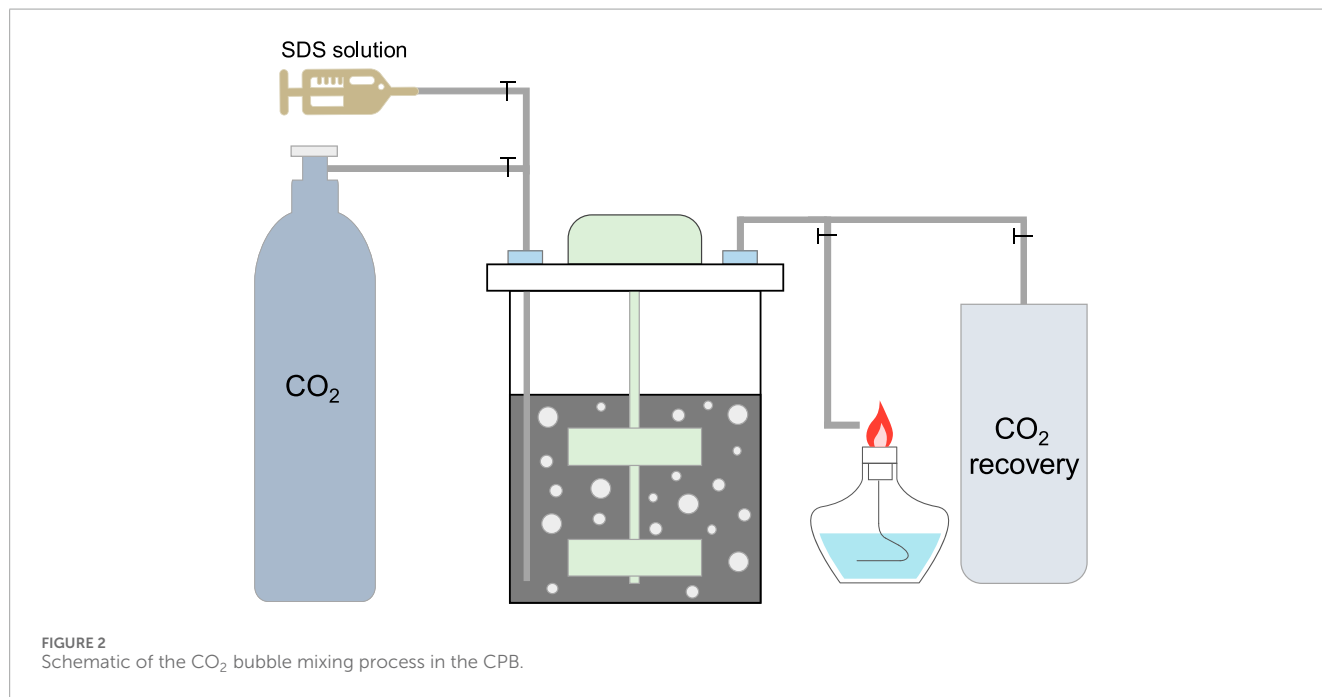


TABLE 3 Mix composition of the prepared specimens with curing information.

Specimen abbreviation	Binder Content (%)	Water/binder by weight	SDS content	Time (h)	Curing temperature (°C)
Yield stress and viscosity development influenced by time					
CO ₂ -CPB-Control	4.5	7.35	0.0‰	0, 0.25, 1, 2	20
CO ₂ -CPB-SDS	4.5	7.35	1.0‰	0, 0.25, 1, 2	20
Effect of SDS content					
CO ₂ -CPB-SDS-0.5	4.5	7.35	0.5‰	0, 0.25, 1, 2	20
CO ₂ -CPB-SDS-1.0	4.5	7.35	1.0‰	0, 0.25, 1, 2	20
CO ₂ -CPB-SDS-1.5	4.5	7.35	1.5‰	0, 0.25, 1, 2	20

2 Experimental program

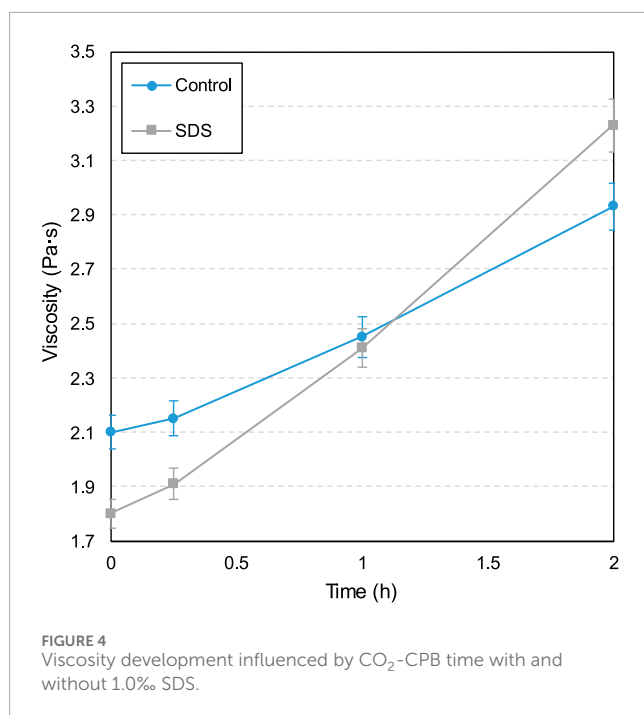
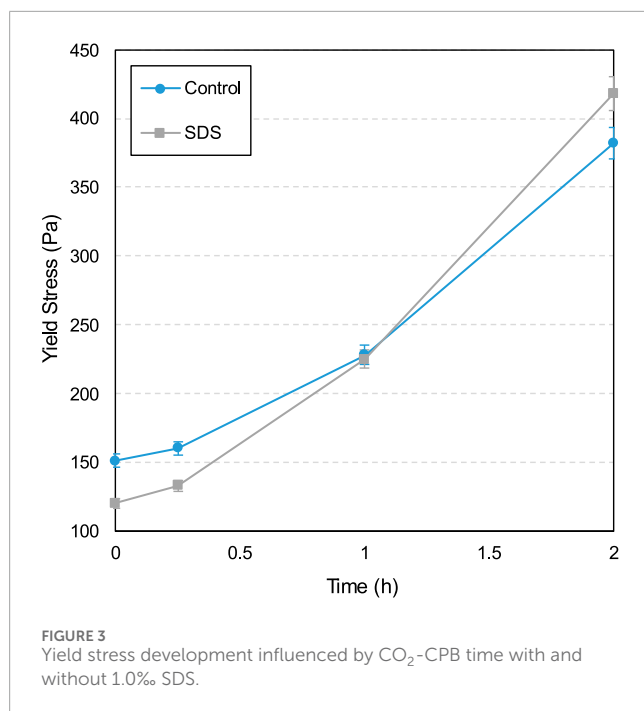
2.1 Materials and mixture proportioning

2.1.1 Materials

The materials used in this study are tailings, binder, air-entraining agent, and water.

2.1.1.1 Tailings

The physical and chemical properties of natural tailings may vary across mines owing to differences in the extracted ore type and mineral processing (Edraki et al., 2014; Falagán et al., 2017; Guo et al., 2023). In this study, silica tailings (STs), containing 99.8 wt% silicon dioxide (SiO₂) and stable in nature, which can significantly reduce the test errors, were used. The particle size



distribution and physical properties of STs were basically the same as the average values of the tailings from ten mines in China, as shown in Figure 1; Table 1. The data information in Figure 1; Table 1 is obtained from the manufacturer, Beijing Silicon Industry Co., Ltd.

2.1.1.2 Binder

Type I silicate cement is the most commonly used binder in mining owing to its good adaptability and stability (Ashraf et al., 2017; Gartner and Sui, 2018; Jiang et al., 2024). The hydration

reaction produces hydrated calcium silicate (C-S-H), calcium aluminate, and AFm (Abdel-Gawwad et al., 2018; Fang et al., 2023; Primus et al., 2019). Additionally, the hydration products harden for increase strength. Type I silicate cement was used in this study, and its specific mineral composition and properties obtained from the manufacturer (Shandong Jiuqi cement Co., Ltd.) are listed in Table 2.

2.1.1.3 Air-entraining agent

In this study, SDS, an anionic surfactant with good foaming properties, was used as a test air-entraining agent (Reales et al., 2018; Zhang et al., 2020). SDS addition produced numerous tiny bubbles in the CPB slurry. In the test, the SDS contents were 0.0%, 0.5%, 1.0%, and 1.5% of the weight of the newly mixed CPB slurry.

2.1.1.4 Water

Ordinary tap water was used to make the backfill slurry.

2.1.2 Specimen preparation and mix proportions

The tailings, cement, and water were mixed in a mixer for 5 min to reach a homogeneous state, and then poured into a closed mixer, as shown in Figure 2. Subsequently, CO₂ gas from a 6–8 MPa gas pressure cylinder was injected into the closed mixer for air removal; when the alcohol lamp was turned off, the closed mixer was filled with CO₂. Then, the CO₂ injection was stopped, and a specific amount of SDS solution was injected. After SDS injection, CO₂ was injected at a rate of 1 L/min, and the CO₂ recovery device was turned on. Simultaneously, the mixer was started and stirred at 200 rpm for 2 min to obtain a CPB slurry with CO₂ bubbles, which was used for subsequent rheological and carbon sequestration tests. During mixing, the CO₂ gas was at normal atmospheric pressure. A flowchart of the mixing of CO₂ bubbles into the CPB is shown in Figure 2. The mixing ratios, SDS contents, curing times, and temperatures are listed in Table 3.

2.2 Test methods

2.2.1 Yield stress test

A vane shear test was conducted to measure the yield stress of the slurry (Wu and Fall 2024). A 27-WF1730/4 instrument model was used, which is easy to operate. In this study, A No. 1 torsion spring and a cross-shaped plate head with a radius of 12.5 mm and height of 25 mm were used. The vane shear test procedure was as follows:

- Clean the cross-plate head of the instrument and set the dial to zero.
- The height of the cross-plate is adjusted such that the bottom of the cross-plate head is immersed from the centre of the sample surface until the top of the cross-plate head is 10–20 mm below the sample surface.
- After 30 s of resting, the pointer reading of the dial is recorded as the initial angle.
- Start the power supply and the inner dial rotates at a fixed speed of 0.18 rpm.
- When the strain indicator is separated from the pointer, the sample fails. The test is stopped, the maximum torque is

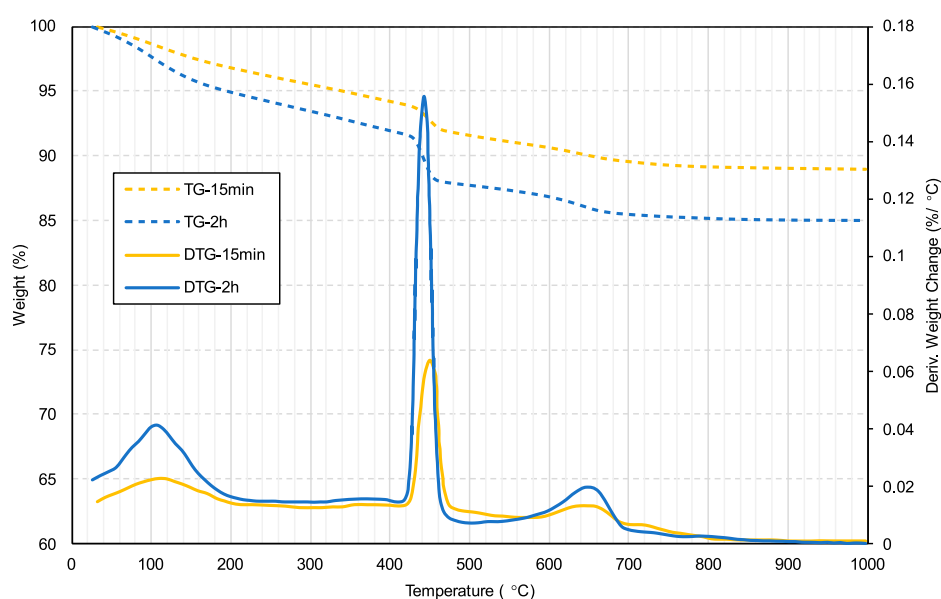


FIGURE 5
TG/DTG curves of the 15-min and 2-h CO_2 -CPB without SDS.

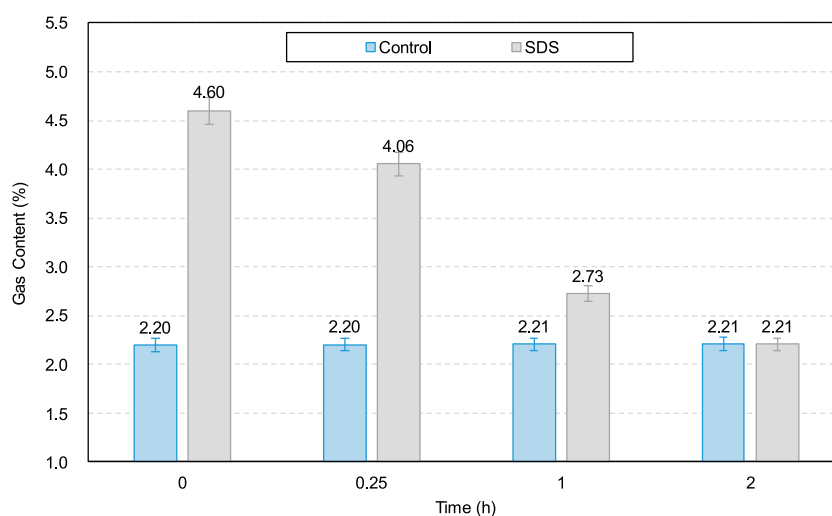


FIGURE 6
Gas content development influenced by CO_2 -CPB time with and without 1.0% SDS.

recorded, and the yield stress of the sample is automatically calculated using a calculation program.

2.2.2 Viscosity test

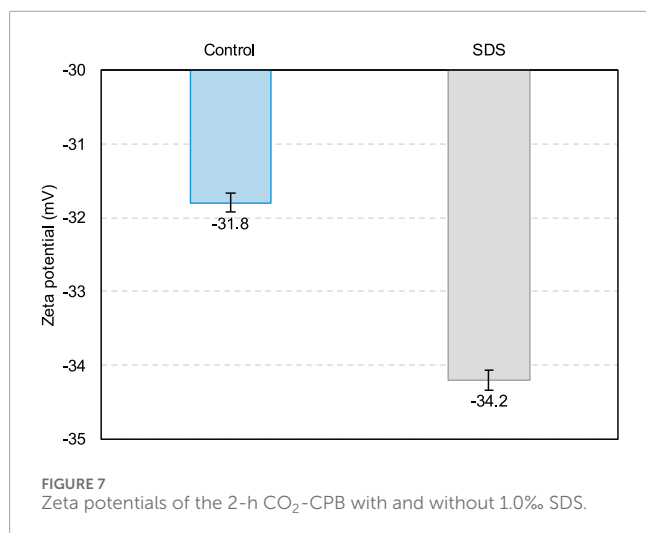
Rotational viscometers are widely used for non-Newtonian fluid viscosity measurements owing to their simplicity, speed, and accuracy (Carnogursky et al., 2023). In this study, a digital rotational viscometer (model DV-E, Brookfield, United States) was used to test the slurry viscosity. The rotor model selected for the experiment was an RV5 with a speed of 50 rpm, which can maintain the measured torque percentage of the slurry in the range of 10%–90% and ensure the accuracy of the obtained viscosity values.

2.2.3 Gas content test

In this study, the slurry gas content affected the rheological properties and efficiency of the CO_2 mineralisation reaction; therefore, a digital display gas content tester (CA-3) was used to measure the slurry gas content. The gas content was measured according to Chinese standard JGJ/T 70-2009. The gas content of each group of samples was tested three times, and the test results are expressed as the arithmetic average of the three measurements.

2.2.4 Microstructural analysis

In this study, a thermogravimetric analyser (Science TG-DTA8122) was used for the thermogravimetric (TG) and differential



thermogravimetric (DTG) analysis of the specimens. Before testing, all specimens were dried at a temperature of 45°C until the sample quality remained constant. During the test, the sample was programmed to heat up in a nitrogen environment (300 mL/min) at a temperature increase of 10°C/min, and the test temperature range was from room temperature to 1,000°C.

2.2.5 Zeta potential measurement

A Zetasizer Nano device was used to measure the zeta potential of the sample, which is calculated by determining the electrophoretic mobility and then applying Henry's equation to calculate the zeta potential. Electrophoretic mobility was obtained by performing electrophoretic experiments on the sample and measuring the velocity of the particles using a laser Doppler velocimeter (LDV) (Clogston and Patri, 2011). The higher the absolute value of the measured zeta potential, the greater the repulsive force between the particles (Roshani and Fall, 2020). In this study, the zeta potential was tested at an ambient temperature of 20°C. Zeta potential measurements were performed at least three times for each sample to minimise errors in the results.

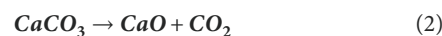
3 Results

3.1 Rheological property development influenced by CO₂-CPB time with and without SDS

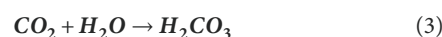
The yield stress and viscosity development influenced according to CO₂-CPB time with and without 1.0‰ SDS are shown in Figures 3, 4, respectively. A sample without SDS was designated as the control sample.

According to the results shown in Figure 3, the yield stress for all specimens exhibits a gradual increase between 0 and 2 h. This gradually increasing yield stress is correlated with the cement hydration degree in the slurry, which increased over time. Figure 5 shows the TG/DTG curves of specimens without SDS after curing for 15 min and 2 h. As can be seen, all samples have three distinct weight loss peaks between 60 and 180, 380–480, and 600°C–800°C.

The weight loss occurring at 60°C–180°C is mainly due to the dehydration reactions of the hydrates, such as C-S-H and ettringite (Rocha et al., 2015; Zhou et al., 2022). The apparent peaks in the second stage (380°C–480°C) are attributed to the de-hydroxylation of the calcium hydroxide (CH) (Gabrovšek et al., 2006; Yilmaz and Fall 2017), as shown in Equation 1. The weight loss in the last stage (600°C–800°C) is due to the decomposition reaction of calcium carbonate (Gaviria et al., 2018; Wang et al., 2024), as shown in Equation 2. As can be seen from Figure 5, all three peaks of the 2-h curve are higher than those of the 15-min curve, indicating that more hydration products (C-S-H, ettringite, and CH) and calcium carbonate are produced at 2 h. In other words, from 0 to 2 h, the products in the sample gradually increased, which led to an increase in the friction resistance between particles, in turn increasing the yield stress (Haiqiang et al., 2016; Malkin et al., 2017).



Additionally, as shown in Figure 3, SDS addition reduced the yield stress of the CO₂-CPB sample for 0–1 h. The lower yield stress of the SDS sample compared to that of the control specimen can be demonstrated by the gas content parameter. The gas content development of the CO₂-CPB samples with and without SDS during 0–2 h is shown in Figure 6. As can be seen, the gas content of the CO₂-CPB sample without SDS remains at approximately 2.2% from 0 to 2 h, whereas SDS addition increases the initial gas content to 4.6%. This increase in gas content is due to the enhanced effect of SDS on the surface activity of the slurry; that is, SDS addition causes the slurry to introduce more CO₂ small bubbles during mixing, resulting in an increase in the gas content of the slurry (Li et al., 2023; Pham and Cramer, 2021; Tunstall et al., 2021). Moreover, as shown in Figure 6, the gas content of CO₂-CPB with SDS gradually decreases from 0 to 1 h because of the reaction of CO₂ gas with the CH generated by cement hydration to produce calcium carbonate (Chen et al., 2022), as shown in Equations 3, 4. In other words, the CO₂ gas in the sample was consumed and converted into solid calcium carbonate particles, resulting in a lower gas content in the slurry. Although the CO₂ gas in the SDS sample was gradually consumed, the gas content of the SDS specimen remained higher than that of the control specimen from 0 to 1 h. However, after 2 h, the gas content of the SDS sample decreased to 2.21% (almost the same as that of the control sample), indicating that the CO₂ gas in the SDS sample was completely consumed at 2 h.



Therefore, according to Figure 6, from 0 to 1 h, the SDS sample exhibits a higher gas content than the control sample, that is, there are more small CO₂ bubbles in the SDS sample, which act as ball lubrication, resulting in a lower yield stress in the SDS specimen (Samson et al., 2017; Yang et al., 2022; Zuo et al., 2023). However, the yield stress of the SDS specimen at 2 h (Figure 3) was higher than that of the control specimen, which does not correspond to a nearly identical gas content at 2 h, as shown in Figure 6. From the zeta

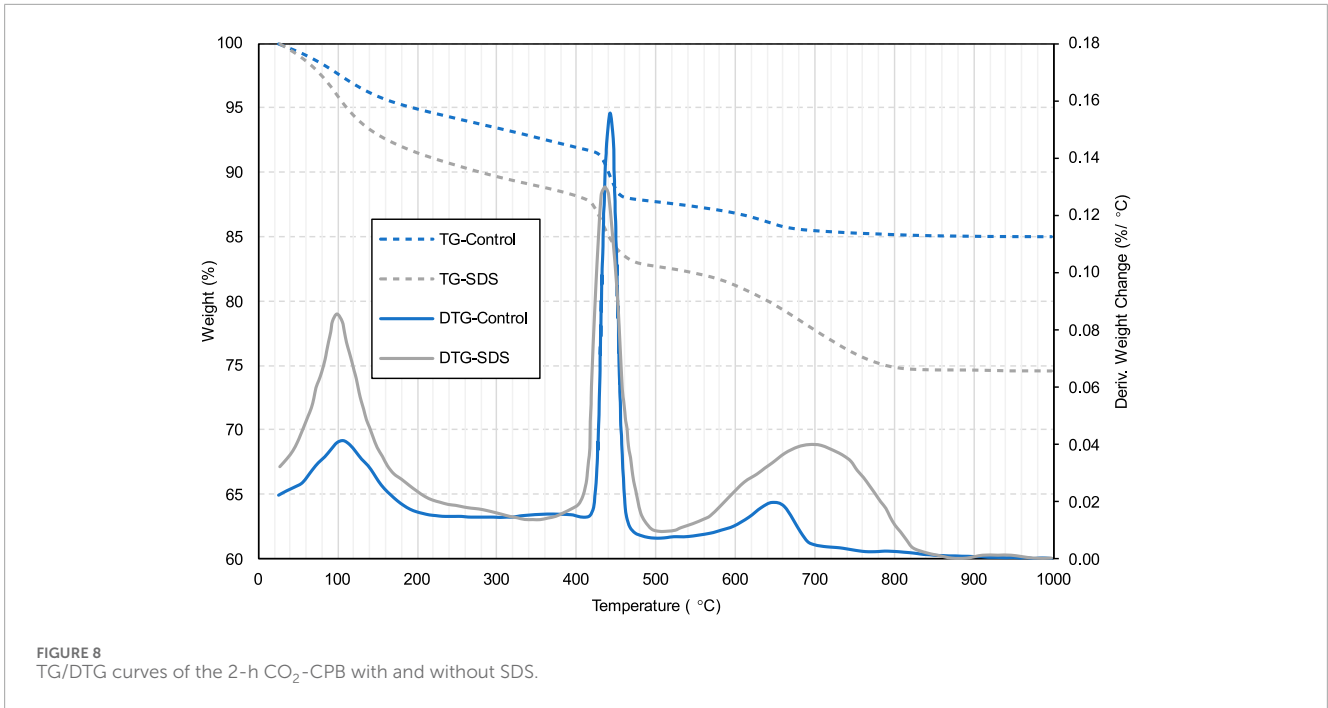


FIGURE 8 TG/DTG curves of the 2-h CO₂-CPB with and without SDS.

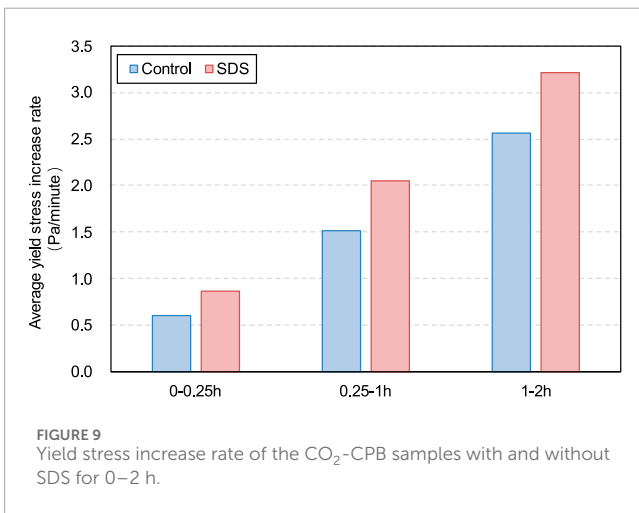


FIGURE 9 Yield stress increase rate of the CO₂-CPB samples with and without SDS for 0–2 h.

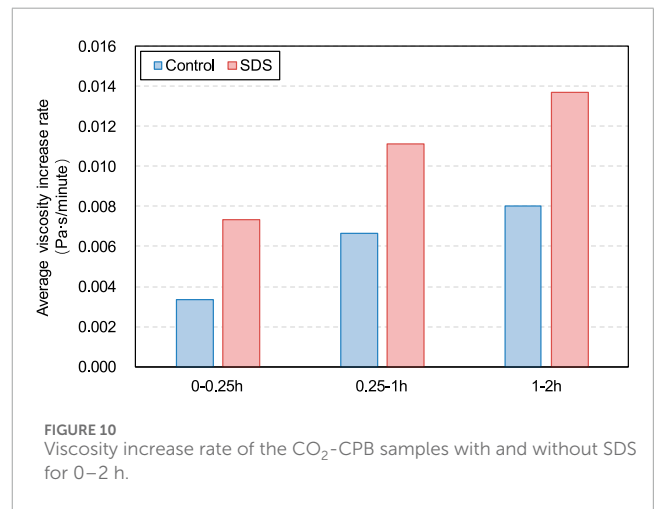
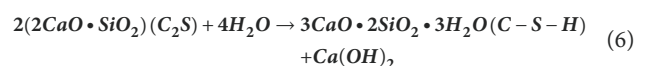
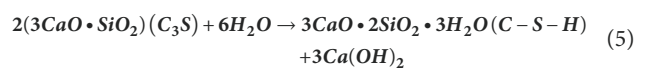


FIGURE 10 Viscosity increase rate of the CO₂-CPB samples with and without SDS for 0–2 h.

potential results at 2 h (Figure 7), the absolute zeta potential value of the SDS specimen was higher than that of the control specimen, indicating greater repulsion between particles in the SDS sample (Elakneswaran et al., 2009; Xiapeng et al., 2019). Previous studies have shown that a greater repulsive force between particles reduces the frictional resistance during flow, thereby reducing the yield stress of the slurry (Simon and Grabinsky, 2013; Xiapeng et al., 2019; Zhou and Fall 2022). Therefore, neither the gas content nor the zeta potential at 2 h could be responsible for the higher yield stress of the SDS sample compared with that of the control sample.

Figure 8 shows the TG/DTG results for the 2-h specimens with and without SDS. As can be seen, the first weight loss peak (60°C–180°C) of the SDS specimen (6.65% weight loss) is higher than that of the control specimen (3.81% weight loss), and the calcium carbonate weight loss peak (600°C–800°C) is also higher

for the former (6.35% weight loss) than for the latter (1.70% weight loss). A greater weight loss indicates that more products (such as C-S-H and calcium carbonate) were generated in the SDS sample. The formation of more C-S-H in the SDS sample is attributed to the presence of CO₂, which consumed the hydration product CH, causing the hydration reaction of the cement (Equations 5, 6) to proceed. On the other hand, as mentioned earlier, the presence of CO₂ bubbles in the SDS sample led to the formation of more calcium carbonate.



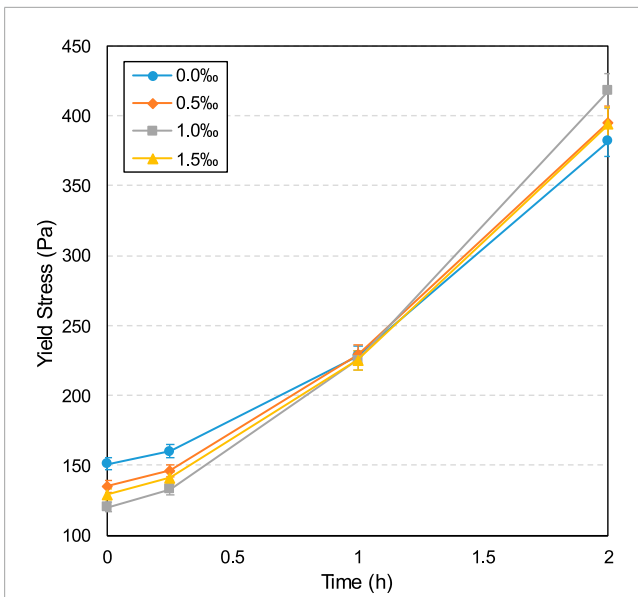


FIGURE 11 Yield stress of the CO₂-CPB with 0.0‰, 0.5‰, 1.0‰, and 1.5‰ SDS for 0, 0.25, 1, and 2 h.

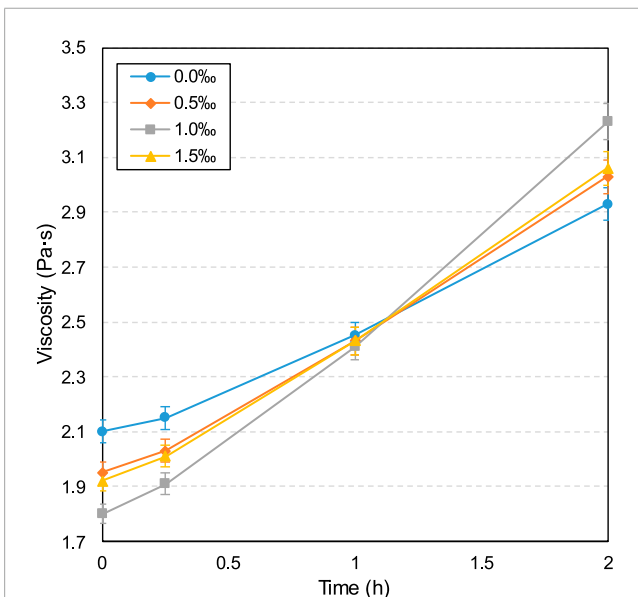


FIGURE 12 Viscosity of the CO₂-CPB with 0.0‰, 0.5‰, 1.0‰, and 1.5‰ SDS for 0, 0.25, 1, and 2 h.

Therefore, the formation of more products in the SDS specimen after 2 h resulted in a higher yield stress than in the control specimen (Figure 3). In summary, compared with the control specimen, there were two competitive factors in the yield stress of the SDS specimen at 2 h: the yield stress reduction effect caused by the increase in the repulsion force between particles and the increase effect caused by the increase in products. According to these results, it can be inferred that the influence of the former is

weaker than that of the latter; therefore, the yield stress of the SDS specimen at 2 h is higher than that of the control specimen.

Furthermore, as can be seen from the viscosity results in Figure 4, the viscosity increases over time for both the control and SDS samples. This viscosity increase over time is due to the hydration reaction progression, that is, the increase in hydration products over time, resulting in greater sample density and frictional resistance between particles, which in turn leads to a tendency for viscosity to increase (Ouattara et al., 2017; Xiao et al., 2021). Additionally, as shown in Figure 4, from 0 to 1 h, the viscosity of the SDS specimen is lower than that of the control specimen. This lower viscosity is due to the larger gas content value shown in Figure 6, that is, the higher the gas content, the lower the slurry density and thus the lower the viscosity (Cao et al., 2022; Şahin et al., 2023). However, the higher viscosity of the SDS sample compared with the control sample at 2 h is due to the formation of more products (such as C-S-H and calcium carbonate) in the SDS sample, as mentioned earlier. In other words, more products lead to a higher sample density, which leads to higher viscosity.

It is worth noting that from 0 to 2 h, both the yield stress and viscosity of the SDS specimen increased at a higher rate compared with the control specimen, as shown in Figures 9, 10. For the SDS samples, this higher yield stress or viscosity growth rate was due to the coincidence of these two factors. First, as previously mentioned, the presence of CO₂ in the SDS sample carbonates CH and promotes the hydration reaction of the cement, leading to the formation of more products and a higher rheological parameter growth rate. Second, CO₂ consumption in the SDS samples leads to a decrease in the internal gas content, resulting in an increase in slurry density, which in turn leads to a larger slurry rheological parameter growth rate than in the control samples.

3.2 Effect of SDS content on the CO₂-CPB rheological properties

Figures 11, 12 show the effects of different SDS contents (0.0‰, 0.5‰, 1.0‰, and 1.5‰) on the CO₂-CPB yield stress and viscosity, respectively. As can be seen, both the yield stress and viscosity increase from 0 to 2 h. The reason for rheological parameter increase with time has been mentioned previously and will not be discussed here for brevity.

Additionally, from 0 to 0.25 h in Figures 11, 12, both the yield stress and viscosity exhibit a decreasing trend as the SDS content increases from 0.0‰ to 1.0‰, which is responsible for the gas content variation in the slurry as the SDS content changes, as shown in Figure 13. As shown in Figure 13, for both the 0- and 0.25-h samples, the gas content exhibits an increasing trend as the SDS content increases from 0.0‰ to 1.0‰. As previously mentioned, a higher gas content leads to a lower slurry density, resulting in a lower yield stress and viscosity. Furthermore, this yield stress and viscosity decrease with increasing SDS content (0.0‰–1.0‰) can also be supported by the zeta potential, as shown in Figure 14. As can be seen, the absolute zeta potential value increases as the SDS content increases from 0.0‰ to 1.0‰, which, as mentioned before, leads to an increase in inter-particle repulsion, resulting in the decrease in yield stress and viscosity.

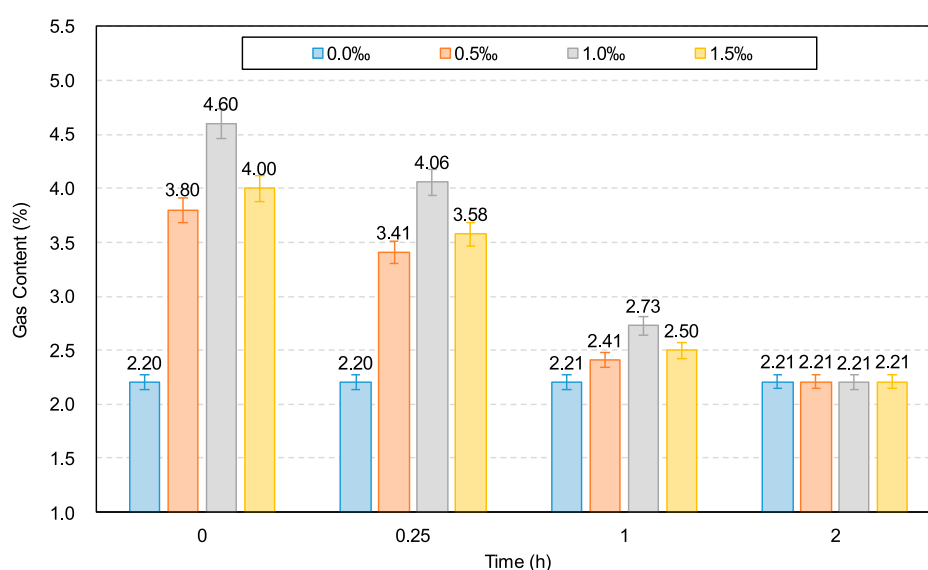


FIGURE 13
Gas content of 0–2-h CO₂-CPB with 0.0‰, 0.5‰, 1.0‰, and 1.5‰ SDS.

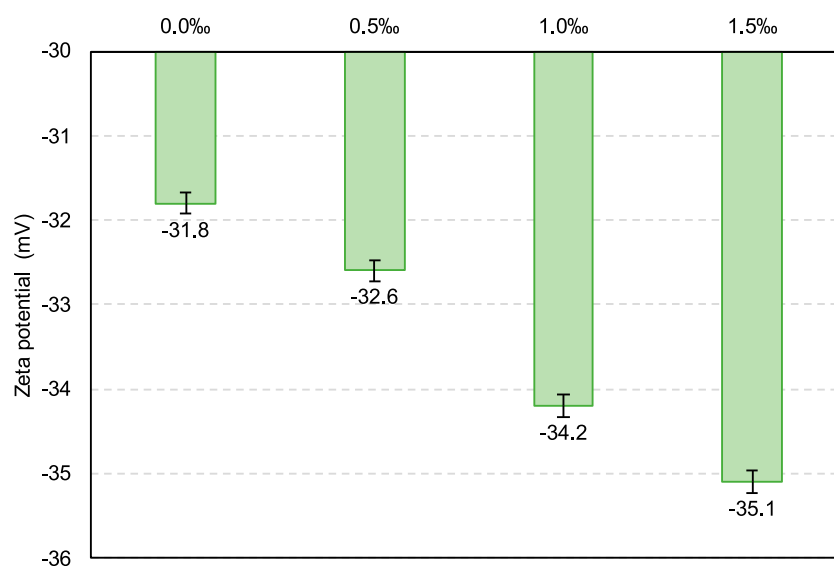


FIGURE 14
Zeta potential of 2-h CO₂-CPB with 0.0‰, 0.5‰, 1.0‰, and 1.5‰ SDS.

However, according to Figures 11, 12, as the SDS content increases from 1.0‰ to 1.5‰, both the yield stress and viscosity of the 0- and 0.25-h samples show an increasing trend. This increasing trend is mainly attributed to the decrease in the gas content of the sample. As shown in Figure 13, as the SDS content increases from 1.0‰ to 1.5‰, the gas content of the 0- and 0.25-h samples shows a decreasing trend, which, as mentioned before, leads to an increase in sample density, resulting in an increase in yield stress and viscosity. Furthermore, as the SDS content increases, the gas content in the slurry exhibits a trend of first increasing and then decreasing, which is consistent with the findings of previous studies (Yang et al., 2022).

In contrast, as shown in Figures 11, 12, samples with 1.0‰ SDS exhibit the highest yield stress and viscosity at 2 h, followed by samples with 0.5‰ and 1.5‰ SDS (similar values), while samples with 0.0‰ SDS exhibit the lowest yield stress and viscosity. This difference in yield stress and viscosity depends mainly on the difference in the amount of products formed in the sample. According to Figure 15, the height of the first and third weight loss peaks is in the following order: 1.0‰ SDS > 1.5‰ SDS > 0.5‰ SDS > 0.0‰ SDS. This is in line with the C-S-H and calcium carbonate amounts in the specimen. As previously mentioned, a greater number of products in the slurry resulted in higher yield stress and viscosity.

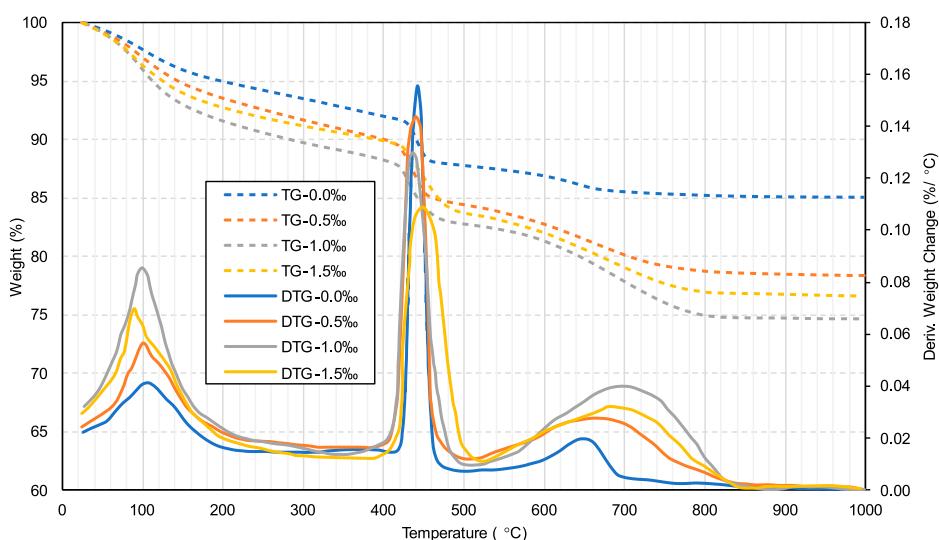


FIGURE 15 TG/DTG curves of the 2-h CO₂-CPB with 0.0%, 0.5%, 1.0%, and 1.5% SDS.

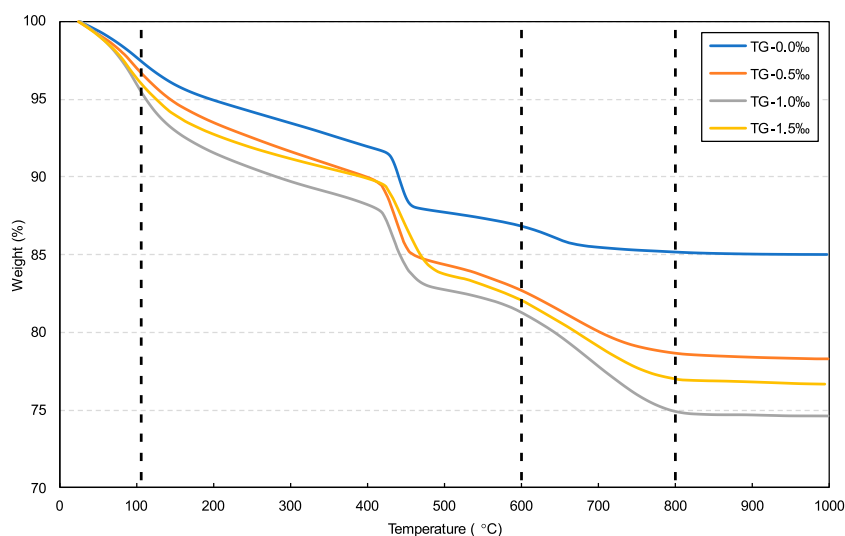


FIGURE 16 TG curves of the 2-h CO₂-CPB with 0.0%, 0.5%, 1.0%, and 1.5% SDS.

3.3 Effect of SDS content on the carbon-sequestration property of the CO₂-CPB

As previously mentioned, the calcium carbonate decomposition weight loss (600°C–800°C) can be measured via thermogravimetric experiments. Therefore, thermogravimetric analysis was adopted in this study to determine the CO₂ uptake ratio of CPB. Based on previous studies (Chen et al., 2022; Moon and Choi, 2019; Park and Choi, 2021) and on the TG curves shown in Figure 16, the CO₂ uptake ratio can be calculated as follows:

$$\text{CO}_2 \text{ uptake} = \frac{\Delta w_{600-800^\circ\text{C}}}{\Delta w_{105^\circ\text{C}}} \times 100\% \quad (7)$$

where $\Delta W_{600-800^\circ\text{C}}$ represents the calcium carbonate decomposition weight loss, and $\Delta W_{105^\circ\text{C}}$ represents the dry weight at 105°C.

The CO₂ uptake ratio of the samples with different SDS contents were calculated using Equation 7, as shown in Figure 17. As can be seen, the CO₂ uptake ratio of the samples with added SDS (0.5%, 1.0%, and 1.5%) is significantly higher than that of the sample without SDS addition (0.0%). This significant increase in the CO₂ uptake ratio is due to the increase in the CO₂ gas content in the slurry caused by SDS addition. As more CO₂ bubbles react with

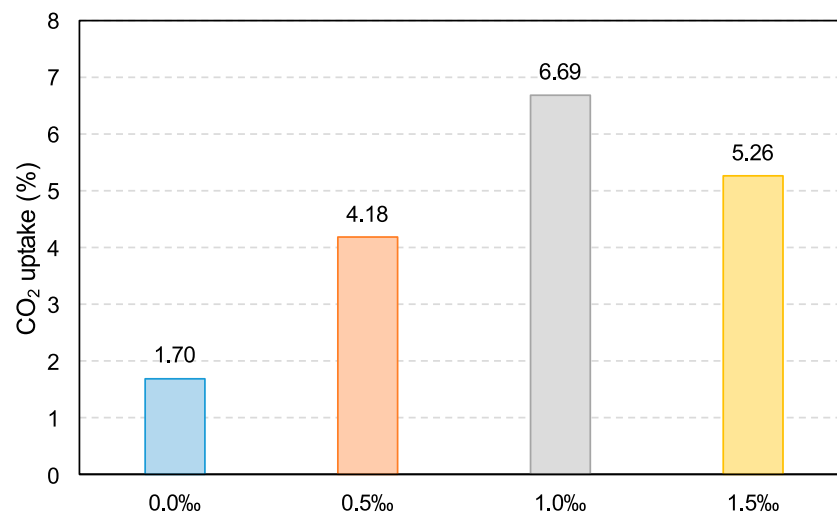


FIGURE 17
CO₂ uptake of the 2-h CO₂-CPB with 0.0‰, 0.5‰, 1.0‰, and 1.5‰ SDS.

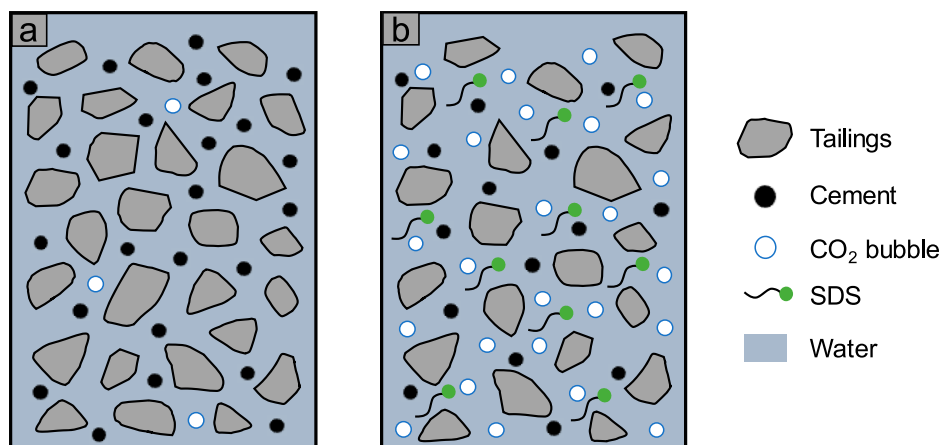


FIGURE 18
Mechanism diagram of SDS in CO₂-CPB. (A) CO₂-CPB without SDS. (B) CO₂-CPB with SDS.

CH to form calcium carbonate, more CO₂ is absorbed by the CPB slurry. Additionally, based on Figure 17, by comparing the results for samples with 0.5‰, 1.0‰, and 1.5‰ SDS, it can be seen that the sample with 1.0‰ SDS has the highest CO₂ uptake ratio, which is confirmed by the test results for the largest gas content of the sample with 1.0‰ SDS, as shown in Figure 13.

From the above analysis, it can be concluded that the CO₂ uptake ratio increases significantly with SDS addition. This indicates that SDS can improve the carbon-sequestration efficiency of the mining backfill industry and has great application value and potential.

4 Discussion

Figure 18 shows the mechanism of SDS in CO₂-CPB. According to this figure, with the addition of SDS, the CO₂ bubbles in the

sample significantly increased, which led to the reduction of yield stress and viscosity of the slurry, that is, the improvement of flow performance (Kim et al., 2021; Mendes et al., 2017). Moreover, the presence of SDS in the slurry led to the increase of the absolute value of zeta potential, that is, the increase of the repulsive force between particles, which also played a positive role in the flow performance of the slurry (Ibrahim and Meawad, 2022; Midekessa et al., 2020).

On the other hand, compared with the slurry without SDS, more CO₂ in the slurry with SDS reacted with CH to form calcium carbonate, which significantly promoted the absorption of CO₂ (Winnefeld et al., 2022; Zajac et al., 2021). This process also caused the hydration reaction to proceed forward to produce more hydration products. Over time, the consumption of CO₂ and the increase in the number of hydration products in the SDS slurry led to an increase in yield stress and viscosity (Ahmed et al., 2009; Rubio-Hernández et al., 2020; Sultangaliyeva et al., 2020).

5 Conclusion

In this study, the influence of SDS on the rheological and carbon-sequestration properties of CO₂-injected CPB slurries were investigated. Based on the results, the main conclusions of this study can be summarized as follows.

- (1) With or without SDS, the yield stress and viscosity of the samples showed a time-dependent increase from 0 to 2 h owing to the increase in products formed over time.
- (2) SDS addition reduced the yield stress and viscosity from 0 to 1 h, but increased the yield stress and viscosity at 2 h. This is mainly related to SDS addition, which resulted in an increase in the gas content from 0 to 1 h and an increase in the products formed at 2 h.
- (3) From 0 to 2 h, the yield stress and viscosity of the SDS specimens increased at a higher rate than those of the control specimen, which is related to the faster rate of product formation and gas content reduction of the SDS specimens compared to those of the control specimen.
- (4) At 0 and 0.25 h, the yield stress and viscosity decreased as the SDS content increased from 0.0‰ to 1.0‰. This is mainly attributed to the increase in the gas content of the slurry and the increase in the absolute zeta potential value. However, as the SDS content increased from 1.0‰ to 1.5‰, the yield stress and viscosity both increased, which is mainly due to the decrease in gas content caused by excessive SDS.
- (5) At 2 h, the order of yield stress and viscosity of the sample is as follows: 1.0‰ SDS > 1.5‰ SDS ≈ 0.5‰ SDS > 0.0‰ SDS. This mainly depended on the differences in the amounts of products formed in the samples.
- (6) The CO₂ uptake ratio of the sample with added SDS (0.5‰, 1.0‰, and 1.5‰) is significantly higher than that of the sample without SDS addition (0.0‰). This significant increase in the CO₂ uptake ratio is attributed to the increase in the CO₂ gas content in the slurry caused by SDS addition, which results in more CO₂ bubbles reacting with CH to form calcium carbonate.

These findings provide effective guidance for improving the carbon-sequestration efficiency of mine backfills and contribute to the promotion of green development in the mining industry.

References

- Abdel-Gawwad, H., Abd El-Aleem, S., Amer, A., El-Didamony, H., and Arif, M. (2018). Combined impact of silicate-amorphicity and MgO-reactivity on the performance of Mg-silicate cement. *Constr. Build. Mater.* 189, 78–85. doi:10.1016/j.conbuildmat.2018.08.171
- Adedoyin, F., Ozturk, I., Abubakar, I., Kumeka, T., Folarin, O., and Bekun, F. V. (2020). Structural breaks in CO₂ emissions: are they caused by climate change protests or other factors? *J. Environ. Manag.* 266, 110628. doi:10.1016/j.jenvman.2020.110628
- Ahmed, R. M., Takach, N., Khan, U., Taoutaou, S., James, S., Saasen, A., et al. (2009). Rheology of foamed cement. *Cem. Concr. Res.* 39 (4), 353–361. doi:10.1016/j.cemconres.2008.12.004
- Ashraf, W., Olek, J., and Jain, J. (2017). Microscopic features of non-hydraulic calcium silicate cement paste and mortar. *Cem. Concr. Res.* 100, 361–372. doi:10.1016/j.cemconres.2017.07.001
- Cao, L., Shi, F., Qiu, M., Chen, W., Cao, P., and Zhou, C. (2022). Effects of air entraining agent on the rheological properties and electrochemical parameters of cement mortar. *Constr. Build. Mater.* 344, 128233. doi:10.1016/j.conbuildmat.2022.128233
- Carnogursky, E. A., Fall, M., and Haruna, S. (2023). Rheology and setting time of saline cemented paste backfill. *Miner. Eng.* 202, 108258. doi:10.1016/j.mineng.2023.108258
- Carvalho, F. P. (2017). Mining industry and sustainable development: time for change. *Food Energy Secur.* 6 (2), 61–77. doi:10.1002/fes3.109

Data availability statement

The original contributions presented in the study are included in the article/supplementary material, further inquiries can be directed to the corresponding author.

Author contributions

ZS: Conceptualization, Formal Analysis, Investigation, Methodology, Writing–original draft. YZ: Supervision, Validation, Writing–review and editing.

Funding

The author(s) declare that no financial support was received for the research, authorship, and/or publication of this article.

Acknowledgments

The authors gratefully acknowledge the support of the Innovation and Development Project of the Information Institution of the Ministry of Emergency Management (Project No. 2024503). The authors would like to thank Shiyanjia Lab (www.shiyanjia.com) for supporting the microstructural tests.

Conflict of interest

The authors declare that the research was conducted in the absence of any commercial or financial relationships that could be construed as a potential conflict of interest.

Publisher's note

All claims expressed in this article are solely those of the authors and do not necessarily represent those of their affiliated organizations, or those of the publisher, the editors and the reviewers. Any product that may be evaluated in this article, or claim that may be made by its manufacturer, is not guaranteed or endorsed by the publisher.

- Cassia, R., Nocioni, M., Correa-Aragunde, N., and Lamattina, L. (2018). Climate change and the impact of greenhouse gases: CO₂ and NO, friends and foes of plant oxidative stress. *Front. Plant Sci.* 9, 273. doi:10.3389/fpls.2018.00273
- Chen, Q., Zhu, L., Wang, Y., Chen, J., and Qi, C. (2022). The carbon uptake and mechanical property of cemented paste backfill carbonation curing for low concentration of CO₂. *Sci. Total Environ.* 852, 158516. doi:10.1016/j.scitotenv.2022.158516
- Clogston, J. D., and Patri, A. K. (2011). Zeta potential measurement. *Charact. nanoparticles Intend. drug Deliv.* 697, 63–70. doi:10.1007/978-1-60327-198-1_6
- Ćwik, A., Casanova, I., Rausis, K., Koukouzas, N., and Zarebska, K. (2018). Carbonation of high-calcium fly ashes and its potential for carbon dioxide removal in coal fired power plants. *J. Clean. Prod.* 202, 1026–1034. doi:10.1016/j.jclepro.2018.08.234
- Edraki, M., Baumgartl, T., Manlapig, E., Bradshaw, D., Franks, D. M., and Moran, C. J. (2014). Designing mine tailings for better environmental, social and economic outcomes: a review of alternative approaches. *J. Clean. Prod.* 84, 411–420. doi:10.1016/j.jclepro.2014.04.079
- Eker, H., and Bascetin, A. (2022). The study of strength behaviour of zeolite in cemented paste backfill. *Geomechanics Eng.* 29 (4), 421–434. doi:10.12989/gae.2022.29.4.421
- Elakneswaran, Y., Nawa, T., and Kurumisawa, K. (2009). Zeta potential study of paste blends with slag. *Cem. Concr. Compos.* 31 (1), 72–76. doi:10.1016/j.cemconcomp.2008.09.007
- Falagán, C., Graill, B. M., and Johnson, D. B. (2017). New approaches for extracting and recovering metals from mine tailings. *Miner. Eng.* 106, 71–78. doi:10.1016/j.mineng.2016.10.008
- Fang, K., Zhang, J., Cui, L., Haruna, S., and Li, M. (2023). Cost optimization of cemented paste backfill: state-of-the-art review and future perspectives. *Miner. Eng.* 204, 108414. doi:10.1016/j.mineng.2023.108414
- Farajzadeh, R., Eftekhari, A. A., Dafnomilis, G., Lake, L., and Bruining, J. (2020). On the sustainability of CO₂ storage through CO₂-Enhanced oil recovery. *Appl. Energy* 261, 114467. doi:10.1016/j.apenergy.2019.114467
- Farjana, S. H., Huda, N., Mahmud, M. P., and Saidur, R. (2019). A review on the impact of mining and mineral processing industries through life cycle assessment. *J. Clean. Prod.* 231, 1200–1217. doi:10.1016/j.jclepro.2019.05.264
- Gabrovšek, R., Vuk, T., and Kaučič, V. (2006). Evaluation of the hydration of Portland cement containing various carbonates by means of thermal analysis. *Acta Chim. Slov.* 53 (2), 159–165.
- Gagné, R. (2016). "Air entraining agents," in *Science and technology of concrete admixtures* (Elsevier), 379–391.
- Gartner, E., and Sui, T. (2018). Alternative cement clinkers. *Cem. Concr. Res.* 114, 27–39. doi:10.1016/j.cemconres.2017.02.002
- Gaviria, X., Borrachero, M. V., Payá, J., Monzó, J. M., and Tobón, J. I. (2018). Mineralogical evolution of cement pastes at early ages based on thermogravimetric analysis (TG). *J. Therm. Analysis Calorim.* 132, 39–46. doi:10.1007/s10973-017-6905-0
- Guo, Z., Qiu, J., Pel, L., Zhao, Y., Zhu, Q., Kwek, J. W., et al. (2023). A contribution to understanding the rheological measurement, yielding mechanism and structural evolution of fresh cemented paste backfill. *Cem. Concr. Compos.* 143, 105221. doi:10.1016/j.cemconcomp.2023.105221
- Haiqiang, J., Fall, M., and Cui, L. (2016). Yield stress of cemented paste backfill in sub-zero environments: experimental results. *Miner. Eng.* 92, 141–150. doi:10.1016/j.mineng.2016.03.014
- Hefni, M., and Hassani, F. (2021). Effect of air entrainment on cemented mine backfill properties: analysis based on response surface methodology. *Minerals* 11 (1), 81. doi:10.3390/min11010081
- Hu, Z., Chen, C., Xiao, W., Wang, X., and Gao, M. (2016). Surface movement and deformation characteristics due to high-intensive coal mining in the windy and sandy region. *Int. J. Coal Sci. & Technol.* 3, 339–348. doi:10.1007/s40789-016-0144-z
- Ibrahim, S., and Meawad, A. (2022). Towards green concrete: study the role of waste glass powder on cement/superplasticizer compatibility. *J. Build. Eng.* 47, 103751. doi:10.1016/j.jobbe.2021.103751
- Ji, L., and Yu, H. (2018). "Carbon dioxide sequestration by direct mineralization of fly ash," in *Carbon dioxide sequestration in cementitious construction materials* (Elsevier), 13–37.
- Jiang, H., Zheng, J., Fu, Y., Wang, Z., Yilmaz, E., and Cui, L. (2024). Slag-based stabilization/solidification of hazardous arsenic-bearing tailings as cemented paste backfill: strength and arsenic immobilization assessment. *Case Stud. Constr. Mater.* 20, e03002. doi:10.1016/j.cscm.2024.e03002
- Khandani, F. S., Atapour, H., Rad, M. Y., and Khosh, B. (2023). An experimental study on the mechanical properties of underground mining backfill materials obtained from recycling of construction and demolition waste. *Case Stud. Constr. Mater.* 18, e02046. doi:10.1016/j.cscm.2023.e02046
- Kim, J.-H., Choi, I.-J., and Chung, C.-W. (2021). Dispersion of single wall carbon nanotube using air entraining agent and its application to portland cement paste. *Constr. Build. Mater.* 302, 124421. doi:10.1016/j.conbuildmat.2021.124421
- Kundu, S., Karmakar, P., Rahaman, S. M., Mitra, M., Rajwar, S., Dhibar, S., et al. (2023). A promising mixed micellar approach to tune the oxidation of isoprenol by diperiodatoargentate (III) in aqueous media. *New J. Chem.* 47 (9), 4364–4373. doi:10.1039/d2nj05120f
- Kundu, S., Layek, M., Mondal, S., Mitra, M., Karmakar, P., Rahaman, S. M., et al. (2024). Insights into the micellar catalysed efficient oxidation of 2- and 3-pentanol by cerium (iv) in a greener medium of SDS and STS. *New J. Chem.* 48 (9), 3804–3812. doi:10.1039/d3nj04667b
- Li, M., Zhou, X., Zhao, J., Qu, S., Wang, P., and Li, G. (2023). Preliminary exploration of a novel high-performance air entraining agent based on sodium dodecyl sulfate added self-made fluorocarbon surfactant. *Constr. Build. Mater.* 370, 130564. doi:10.1016/j.conbuildmat.2023.130564
- Lippiatt, N., Ling, T.-C., and Pan, S.-Y. (2020). Towards carbon-neutral construction materials: carbonation of cement-based materials and the future perspective. *J. Build. Eng.* 28, 101062. doi:10.1016/j.jobbe.2019.101062
- Lu, G., Selvadurai, P., and Meguid, M. A. (2024). Analytical solution to non-isothermal pore-pressure evolution in hydrating minefill. *Can. Geotech. J. (jg)*. doi:10.1139/cgj-2023-0464
- Ma, L., Xu, Y., Ngo, I., Wang, Y., Zhai, J., and Hou, L. (2022). Prediction of water-blocking capability of water-seepage-resistance strata based on AHP-fuzzy comprehensive evaluation method—a case study. *Water* 14 (16), 2517. doi:10.3390/w14162517
- Malkin, A., Kulichikhin, V., and Ilyin, S. (2017). A modern look on yield stress fluids. *Rheol. Acta* 56, 177–188. doi:10.1007/s00397-016-0963-2
- Marimuthu, R., Sankaranarayanan, B., Ali, S. M., de Sousa Jabbour, A. B. L., and Karupiah, K. (2021). Assessment of key socio-economic and environmental challenges in the mining industry: implications for resource policies in emerging economies. *Sustain. Prod. Consum.* 27, 814–830. doi:10.1016/j.spc.2021.02.005
- Markiv, T. (2022). Properties of fresh and hardened mortars with air-entraining agent. *Theory Build. Pract.* 2022 (2), 105–110. doi:10.23939/jtbp2022.02.105
- Mendes, J. C., Moro, T. K., Figueiredo, A. S., do Carmo Silva, K. D., Silva, G. C., Silva, G. J. B., et al. (2017). Mechanical, rheological and morphological analysis of cement-based composites with a new LAS-based air entraining agent. *Constr. Build. Mater.* 145, 648–661. doi:10.1016/j.conbuildmat.2017.04.024
- Midekessa, G., Godakumara, K., Ord, J., Viil, J., Lattekivi, F., Dissanayake, K., et al. (2020). Zeta potential of extracellular vesicles: toward understanding the attributes that determine colloidal stability. *ACS omega* 5 (27), 16701–16710. doi:10.1021/acsomega.0c01582
- Mo, L., Zhang, F., Deng, M., and Panesar, D. K. (2016). Effectiveness of using CO₂ pressure to enhance the carbonation of Portland cement-fly ash-MgO mortars. *Cem. Concr. Compos.* 70, 78–85. doi:10.1016/j.cemconcomp.2016.03.013
- Mohsin, M., Zhu, Q., Naseem, S., Sarfraz, M., and Ivascu, L. (2021). Mining industry impact on environmental sustainability, economic growth, social interaction, and public health: an application of semi-quantitative mathematical approach. *Processes* 9 (6), 972. doi:10.3390/pr9060972
- Moon, E.-J., and Choi, Y. C. (2019). Carbon dioxide fixation via accelerated carbonation of cement-based materials: potential for construction materials applications. *Constr. Build. Mater.* 199, 676–687. doi:10.1016/j.conbuildmat.2018.12.078
- Ngo, I., Ma, L., Zhai, J., and Wang, Y. (2023). Enhancing fly ash utilization in backfill materials treated with CO₂ carbonation under ambient conditions. *Int. J. Min. Sci. Technol.* 33 (3), 323–337. doi:10.1016/j.ijmst.2023.02.001
- Olajire, A. A. (2013). A review of mineral carbonation technology in sequestration of CO₂. *J. Petroleum Sci. Eng.* 109, 364–392. doi:10.1016/j.petrol.2013.03.013
- Ouattara, D., Yahia, A., Mbonimpa, M., and Belem, T. (2017). Effects of superplasticizer on rheological properties of cemented paste backfills. *Int. J. Min. Process* 161, 28–40. doi:10.1016/j.minpro.2017.02.003
- Ouyang, X., Guo, Y., and Qiu, X. (2008). The feasibility of synthetic surfactant as an air entraining agent for the cement matrix. *Constr. Build. Mater.* 22 (8), 1774–1779. doi:10.1016/j.conbuildmat.2007.05.002
- Park, B., and Choi, Y. C. (2021). Investigation of carbon-capture property of foam concrete using stainless steel AOD slag. *J. Clean. Prod.* 288, 125621. doi:10.1016/j.jclepro.2020.125621
- Pham, L. T., and Cramer, S. M. (2021). Effects of air-entraining admixtures on stability of air bubbles in concrete. *J. Mater. Civ. Eng.* 33 (4), 04021018. doi:10.1061/(asce)mt.1943-5533.0003628
- Primus, C. M., Tay, F. R., and Niu, L.-n. (2019). Bioactive tri/dicalcium silicate cements for treatment of pulpal and periapical tissues. *Acta biomater.* 96, 35–54. doi:10.1016/j.actbio.2019.05.050
- Qi, C.-c. (2020). Big data management in the mining industry. *Metallurgy Mater.* 27 (2), 131–139. doi:10.1007/s12613-019-1937-z
- Reales, O. A. M., Jaramillo, Y. P. A., Botero, J. C. O., Delgado, C. A., Quintero, J. H., and Toledo Filho, R. D. (2018). Influence of MWCNT/surfactant dispersions on the rheology of Portland cement pastes. *Cem. Concr. Res.* 107, 101–109. doi:10.1016/j.cemconres.2018.02.020

- Rocha, C. A. A., Cordeiro, G. C., and Toledo Filho, R. D. (2015). Use of thermal analysis to determine the hydration products of oil well cement pastes containing NaCl and KCl. *J. Therm. Analysis Calorim.* 122, 1279–1288. doi:10.1007/s10973-015-4949-6
- Roshani, A., and Fall, M. (2020). Rheological properties of cemented paste backfill with nano-silica: link to curing temperature. *Cem. Concr. Compos.* 114, 103785. doi:10.1016/j.cemconcomp.2020.103785
- Rubio-Hernández, F., Adarve-Castro, A., Velázquez-Navarro, J., Páez-Flor, N., and Delgado-García, R. (2020). Influence of water/cement ratio, and type and concentration of chemical additives on the static and dynamic yield stresses of Portland cement paste. *Constr. Build. Mater.* 235, 117744. doi:10.1016/j.conbuildmat.2019.117744
- Şahin, H. G., Mardani, A., Özen, S., and Emin, A. (2023). Utilization of high-range water reducing admixture having air-entraining agents in cementitious systems. *J. Build. Eng.* 64, 105565. doi:10.1016/j.jobbe.2022.105565
- Samson, G., Phelipot-Mardelé, A., Lanos, C., and Pierre, A. (2017). Quasi-static bubble in a yield stress fluid: elasto-plastic model. *Rheol. Acta* 56, 431–443. doi:10.1007/s00397-017-1007-2
- Sánchez, F., and Hartlieb, P. (2020). Innovation in the mining industry: technological trends and a case study of the challenges of disruptive innovation. *Min. Metallurgy & Explor.* 37 (5), 1385–1399. doi:10.1007/s42461-020-00262-1
- Sari, M., Yilmaz, E., Kasap, T., and Karasu, S. (2023). Exploring the link between ultrasonic and strength behavior of cementitious mine backfill by considering pore structure. *Constr. Build. Mater.* 370, 130588. doi:10.1016/j.conbuildmat.2023.130588
- Sheshpari, M. (2015). A review of underground mine backfilling methods with emphasis on cemented paste backfill. *Electron. J. Geotechnical Eng.* 20 (13), 5183–5208.
- Simon, D., and Grabinsky, M. (2013). Apparent yield stress measurement in cemented paste backfill. *Int. J. Min. Reclam. Environ.* 27 (4), 231–256. doi:10.1080/17480930.2012.680754
- Solismaa, S., Torppa, A., Kuva, J., Heikkilä, P., Hyvönen, S., Juntunen, P., et al. (2021). Substitution of cement with granulated blast furnace slag in cemented paste backfill: evaluation of technical and chemical properties. *Minerals* 11 (10), 1068. doi:10.3390/min11101068
- Song, X., Yu, X., Zhao, W., Yang, F., Shi, J., and Yalçınkaya, Ç. (2023). Progressive damage process and destabilization precursor recognition of sulfate tailing-cemented paste backfill based on acoustic emission. *Powder Technol.* 430, 119047. doi:10.1016/j.powtec.2023.119047
- Sultangaliyeva, F., Carré, H., La Borderie, C., Zuo, W., Keita, E., and Roussel, N. (2020). Influence of flexible fibers on the yield stress of fresh cement pastes and mortars. *Cem. Concr. Res.* 138, 106221. doi:10.1016/j.cemconres.2020.106221
- Sun, W., Wang, H., and Hou, K. (2018). Control of waste rock-tailings paste backfill for active mining subsidence areas. *J. Clean. Prod.* 171, 567–579. doi:10.1016/j.jclepro.2017.09.253
- Thompson, B. D., Bawden, W. F., and Grabinsky, M. (2012). *In situ* measurements of cemented paste backfill at the Cayeli Mine. *Can. Geotech. J.* 49 (7), 755–772. doi:10.1139/t2012-040
- Tunstall, L. E., Ley, M. T., and Scherer, G. W. (2021). Air entraining admixtures: mechanisms, evaluations, and interactions. *Cem. Concr. Res.* 150, 106557. doi:10.1016/j.cemconres.2021.106557
- Tuokuu, F. X. D., Idemudia, U., Gruber, J. S., and Kayira, J. (2019). Identifying and clarifying environmental policy best practices for the mining industry—a systematic review. *J. Clean. Prod.* 222, 922–933. doi:10.1016/j.jclepro.2019.03.111
- Uliasz-Bocheńczyk, A., and Mokrzycki, E. (2020). The potential of FBC fly ashes to reduce CO₂ emissions. *Sci. Rep.* 10 (1), 9469. doi:10.1038/s41598-020-66297-y
- Unluer, C. (2018). “Carbon dioxide sequestration in magnesium-based binders,” in *Carbon dioxide sequestration in cementitious construction materials* (Elsevier), 129–173.
- Wang, P., Mao, X., and Chen, S.-E. (2019). CO₂ sequestration characteristics in the cementitious material based on gangue backfilling mining method. *Int. J. Min. Sci. Technol.* 29 (5), 721–729. doi:10.1016/j.ijmst.2019.03.005
- Wang, X., Guo, J., Wu, A., Wang, H., Jiang, H., Li, Z., et al. (2024). Wear characteristics of the pipeline transporting cemented paste backfill containing coarse aggregate. *Constr. Build. Mater.* 410, 134170. doi:10.1016/j.conbuildmat.2023.134170
- Wilson, J. C., Benbow, S., and Metcalfe, R. (2018). Reactive transport modelling of a cement backfill for radioactive waste disposal. *Cem. Concr. Res.* 111, 81–93. doi:10.1016/j.cemconres.2018.06.007
- Winnefeld, F., Leemann, A., German, A., and Lothenbach, B. (2022). CO₂ storage in cement and concrete by mineral carbonation. *Curr. Opin. Green Sustain. Chem.* 38, 100672. doi:10.1016/j.cogsc.2022.100672
- Wu, F., and Fall, M. (2024). Sulphate-temperature-time interactions and their influence on rheological characteristics of cemented paste backfill. *Powder Technol.* 440, 119741. doi:10.1016/j.powtec.2024.119741
- Xiao, B., Fall, M., and Roshani, A. (2021). Towards understanding the rheological properties of slag-cemented paste backfill. *Int. J. Min. Reclam. Environ.* 35 (4), 268–290. doi:10.1080/17480930.2020.1807667
- Xiapeng, P., Fall, M., and Haruna, S. (2019). Sulphate induced changes of rheological properties of cemented paste backfill. *Miner. Eng.* 141, 105849. doi:10.1016/j.mineng.2019.105849
- Xu, Y., and Ma, L. (2024). Characteristics of overburden migration under continuous extraction and continuous backfill mining method with CO₂ mineralized filling materials. *J. Clean. Prod.* 440, 140920. doi:10.1016/j.jclepro.2024.140920
- Yamada, H. (2021). Amine-based capture of CO₂ for utilization and storage. *Polym. J.* 53 (1), 93–102. doi:10.1038/s41428-020-00400-y
- Yang, B., Wang, X., Yin, P., Gu, C., Yin, X., Yang, F., et al. (2022). The rheological properties and strength characteristics of cemented paste backfill with air-entraining agent. *Minerals* 12 (11), 1457. doi:10.3390/min12111457
- Yilmaz, E. (2023). Innovative mine backfill materials and structures. *International Journal of Mining, Reclamation and Environment* 37 (10), 731–734. doi:10.1080/17480930.2023.2293388
- Yilmaz, E., and Fall, M. (2017). Paste tailings management.
- Yin, S., Yan, Z., Chen, X., Yan, R., Chen, D., Chen, J., et al. (2023). Active roof-contact: the future development of cemented paste backfill. *Constr. Build. Mater.* 370, 130657. doi:10.1016/j.conbuildmat.2023.130657
- Zajac, M., Skocek, J., Skibsted, J., and Ben Haha, M. (2021). CO₂ mineralization of demolished concrete wastes into a supplementary cementitious material—a new ccu approach for the cement industry. *RILEM Technical Letters*, 6, 53–60. doi:10.21809/rilemtechlett.2021.141
- Zhang, J., Ke, Y., Zhang, J., Han, Q., and Dong, B. (2020). Cement paste with well-dispersed multi-walled carbon nanotubes: mechanism and performance. *Constr. Build. Mater.* 262, 120746. doi:10.1016/j.conbuildmat.2020.120746
- Zhou, J., Liu, L., Zhao, Y., Zhu, M., Zhuang, D., Zhao, Y., et al. (2024). Mechanism of air-entraining agent to improve the properties of coal-based solid waste backfill. *J. Mater. Res. Technol.* 32, 2140–2148. doi:10.1016/j.jmrt.2024.08.051
- Zhou, Y., and Fall, M. (2022). Investigation on rheological properties of cemented pastefill with chloride-bearing antifreeze additives in sub-zero environments. *Cold Regions Sci. Technol.* 196, 103506. doi:10.1016/j.coldregions.2022.103506
- Zhou, Y., Fall, M., and Haruna, S. (2022). Flow ability of cemented paste backfill with chloride-free antifreeze additives in sub-zero environments. *Cem. Concr. Compos.* 126, 104359. doi:10.1016/j.cemconcomp.2021.104359
- Zuo, S., Yuan, Q., Huang, T., Wang, Z., Zhang, K., and Liu, J. (2023). Rheology and air entrainment of fresh Portland cement mortars in simulated low air pressure environments. *Cem. Concr. Compos.* 135, 104848. doi:10.1016/j.cemconcomp.2022.104848